Available online at www.sciencedirect.com
SCIENCE DIRECT®
Sensors and Actuators A 117 (2005) 309–316
SENSORS AND ACTUATORS A PHYSICAL
www.elsevier.com/locate/sna

Interfaces friction effect of sliding contact on nanoindentation test

Chingfu Tsou[a,*], Changchun Hsu[b], Weileun Fang[b]

[a] *Department of Automatic Control Engineering, Feng Chia University, Taichung, Taiwan, ROC*
[b] *Department of Power Mechanical Engineering, National Tsing Hua University, Hsinchu, Taiwan, ROC*

Received 24 June 2004; accepted 27 June 2004
Available online 7 August 2004

Abstract

The nanoindenation testing system has been extensively applied to determine mechanical properties of thin film presently. However, the contact surface between the indenter and the thin film may arise a sliding friction. The existing report ignores such a friction force effect at the contact surface. This study will present several experimental results to demonstrate the existing of the friction force between the tip of the indenter and the test sample. In this regard, the effect of the sliding friction on thin film mechanical property measurement will be discussed. According to the experiment results, the friction force effect is influenced by the indent depth. In addition, the interface friction force is more significant for the brittle material due to its larger elastic restoring force. The ignorance of the friction effect may lead to significant error when extracting elastic modulus of thin films from the indentation test.

Keywords: Nanoindenation; Thin film; Mechanical properties; Friction force

1. Introduction

The mechanical properties of thin film materials gradually attract a lot of attention for the area of MEMS and IC. The thin film mechanical properties not only affect the mechanical performance but also the electrical as well as the optical performances of the devices. The mechanical property of thin film materials may not be the same as that of the bulk ones. Moreover, the mechanical properties of thin film materials are usually vary with the fabrication processes, film thickness, etc. Various techniques regarding the determining of thin film mechanical properties have been reported in [1–3].

Presently the nanoindenation system has been extensively used for measuring mechanical properties of thin film. The nanoindentation technique has several advantages over other methods. For instance, it is convenient to prepare the sample for nanoindentation test. The online wafer level test is available using the nanoindentation system. In addition, the distribution of the thin film mechanical properties on the wafer surface can be characterized. Further, the load–deflection test is available on the free-standing micromachined cantilever, microbridge, membranes, etc. Thus, it is possible to characterize the mechanical properties such as the stiffness, fracture toughness and the residual stress of the micromachined structures [4–8].

Despite the popularity and practical importance of the nanoindentation technique, various effects that were ignored in the existing technique need to be further studied [9–12]. For instance, the sliding friction between the test film and the indenter was not considered in the existing analytical model. This research aims to study the sliding friction effect occurred on the contact interface between indenters and thin film as show in Fig. 1. Four different samples were employed to demonstrate and discuss the effect of the sliding friction on the characterizing of thin film mechanical properties.

2. Theory of indentation technique

In this study, experiments were performed using a commercial nanoindention system [3,13]. The variation of the

* Corresponding author. Tel.: +886 4 2451 7250; fax: +886 4 42451 9951.
E-mail address: cftsou@fcu.edu.tw (C. Tsou).

0924-4247/$ – see front matter © 2004 Elsevier B.V. All rights reserved.
doi:10.1016/j.sna.2004.06.030

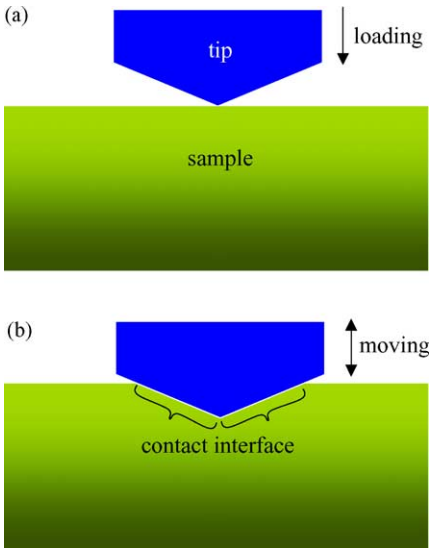

Fig. 1. The sliding friction effect occurred on the contact interface between indenters and thin film.

elastic modulus at different indent depth was used to demonstrate the existing of interface friction effect. As illustrated in Fig. 2, the commercial nanoindentation system is mainly consisted of a magnetic loading actuator, a capacitive displacement sensor, a probe, and supporting springs. A typical load–displacement curve is demonstrated in Fig. 3. As the indenter is driven into the material, both elastic and plastic deformation caused the formation of a hardness impression conforming to the shape of the indenter to some contact depth, h_c. As the indent is withdrawn, only the elastic portion of the displacement is recovered. According to the recovery of the material, the elastic modulus is determined. As reported in [3,13], a so-called reduced modulus is expressed as

$$E_r = \frac{\sqrt{\pi}\, S}{2\beta\sqrt{A}} \tag{1}$$

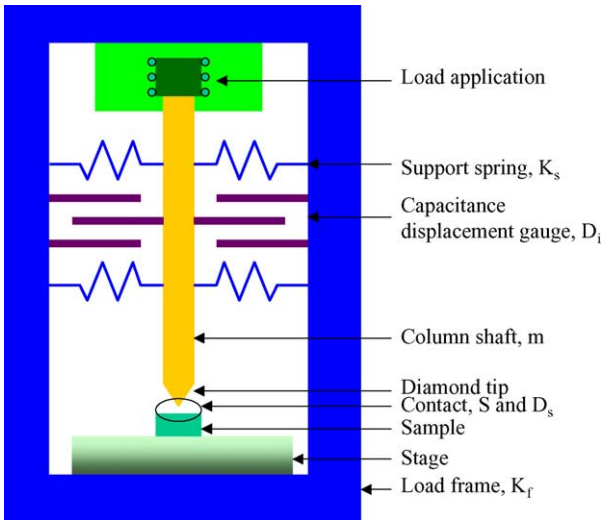

Fig. 2. Schematic diagram of nanoindentation system.

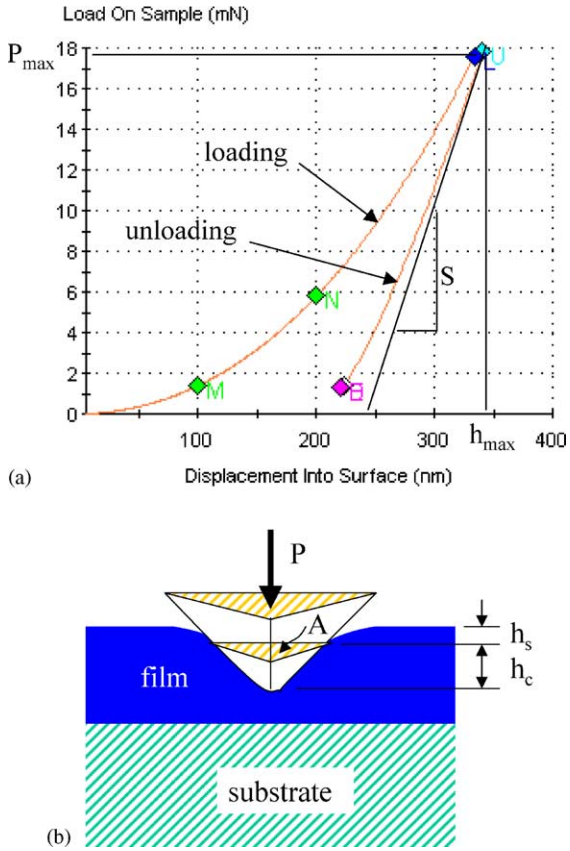

Fig. 3. A typical load–displacement curve.

where A is the projected contact area at that load and β is a constant that depends only the geometry of the indenter. In addition, the stiffness of the sample during contact S (dP/dh) is the slop of the initial portion of the unloading curve indicated in Fig. 3a. The elastic modulus of the test material, E, is expressed as

$$\frac{1}{E_r} = \frac{(1-\upsilon^2)}{E} - \frac{(1-\upsilon_i^2)}{E_i} \tag{2}$$

where υ is the Poisson's ratio of the test material; and E_i and υ_i are the elastic modulus and Poisson's ratio, respectively, of the indenter.

In addition to the static load–deflection test, the material properties can be determined by using the dynamic harmonic excitation test of this commercial indentation system. The existing dynamic model of the indentation system and sample contact [13–15] is illustrated in Fig. 4. The equivalent mass m, spring constant K, and damping coefficient C are contributed from the indentation system and the sample during test. The dynamic response of the system under a harmonic excitation $F_0 \sin \omega t$ can be expressed as

$$m\ddot{z} + D\dot{z} + Kz = F_0 \sin \omega t \tag{3}$$

As indicated in Fig. 2, the equivalent stiffness K is influenced by the stiffness of the sample S during contact, the

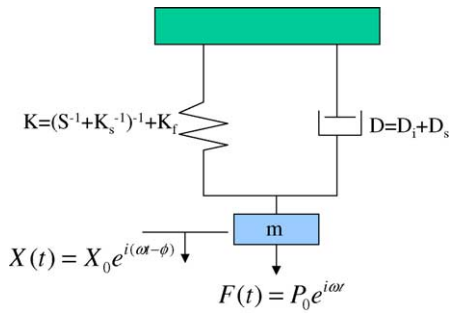

Fig. 4. The existing dynamic model of the indentation system and sample contact.

stiffness of the load frame K_f, and the stiffness of the suspension K_s. Moreover, the equivalent damping D contains the effects contributed from the damping of the sample D_s during contact and the damping of the displacement sensor D_i. Accordingly, the stiffness S and the damping coefficient D_s of the sample during contact can be expressed as

$$S = \left[\frac{1}{F_0/z_0\ \cos\ \phi - (K_s - m\omega^2)} - \frac{1}{K_f}\right] \tag{4}$$

$$D_s\omega = \frac{F_0}{z_0}\sin\ \phi - D_i\omega \tag{5}$$

where z_0 is the measured amplitude of the dynamic response associated with the driving frequency. Since the parameters K_f, m, K_s, and D_i of the system are known in advance; the parameters S and $D_s\omega$ can be determined under a given harmonic excitation $F_0 \sin \omega t$. In this regard, the reduced modulus E_r and the elastic modulus E of the test sample can be determined from Eqs. (1) and (2).

3. Experiment and results

Fig. 2 shows the schematic diagram of the system used to test the thin film in this study. The system employs an XY stage to position the sample directly underneath the tip of the probe. After driven downward by the loading actuator, the probe will indent a notch in the film surface. A force transducer measures the magnitude of the reaction force with the resolution within ±1 nN, and the magnitude of the displacement is measured by capacitive displacement sensor with the resolution within ±0.0002 nm. The Berkovich indenter with a triangular pyramid tip was used in all experiments. The materials are characterized by continuously recording the displacement and load during the indentation process.

There are four thin film materials, including silicon dioxide (SiO_2), silicon nitride (Si_3N_4), aluminum (Al), and nickel (Ni), used to study the contact friction effect of indentation test. Among these materials, the SiO_2, Si_3N_4, and Si are regarded as brittle materials; on the other hand, the Ni and Al are ductile materials. These thin film materials were grown or deposited on (100) silicon wafer. The conditions of these

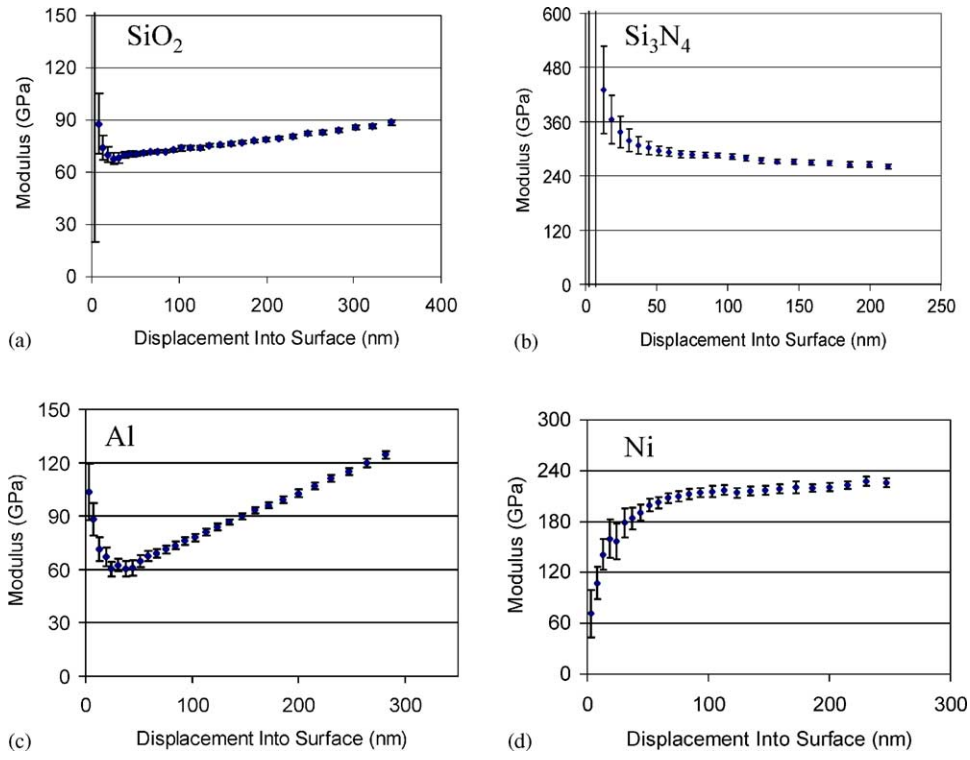

Fig. 5. The elastic modulus of the thin film materials for various different thicknesses.

Table 1
The fabrication processes and thickness of the four different films used in this study

Material	Fabrication	Thickness (μm)
SiO_2	Wet-thermal	0.98
Si_3N_4	LPCVD	0.8
Al	Evaporation	1
Ni	Evaporation	1

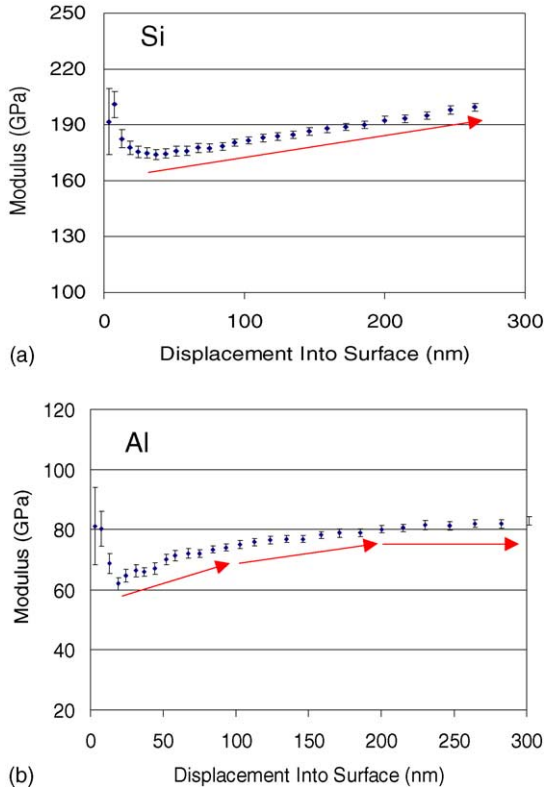

Fig. 6. The experiment results for bulk materials.

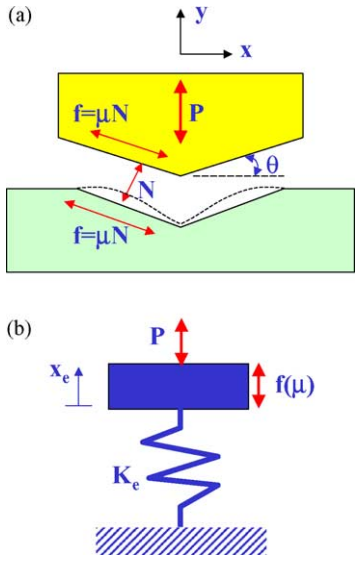

Fig. 7. A physical model for indentation interface.

thin films are listed in Table 1. Moreover, the indentation tests on two bulk materials, including a 500 μm thick single crystal silicon wafer and a 2000 μm thick aluminum, were performed as well.

In this study, experiments were performed using a commercial nanoindention system with 0.0002 nm displacement resolution and 1 nN force resolution. The commercial indentation system will continuously record the load and displacement of the indenter head during the thin film indentation

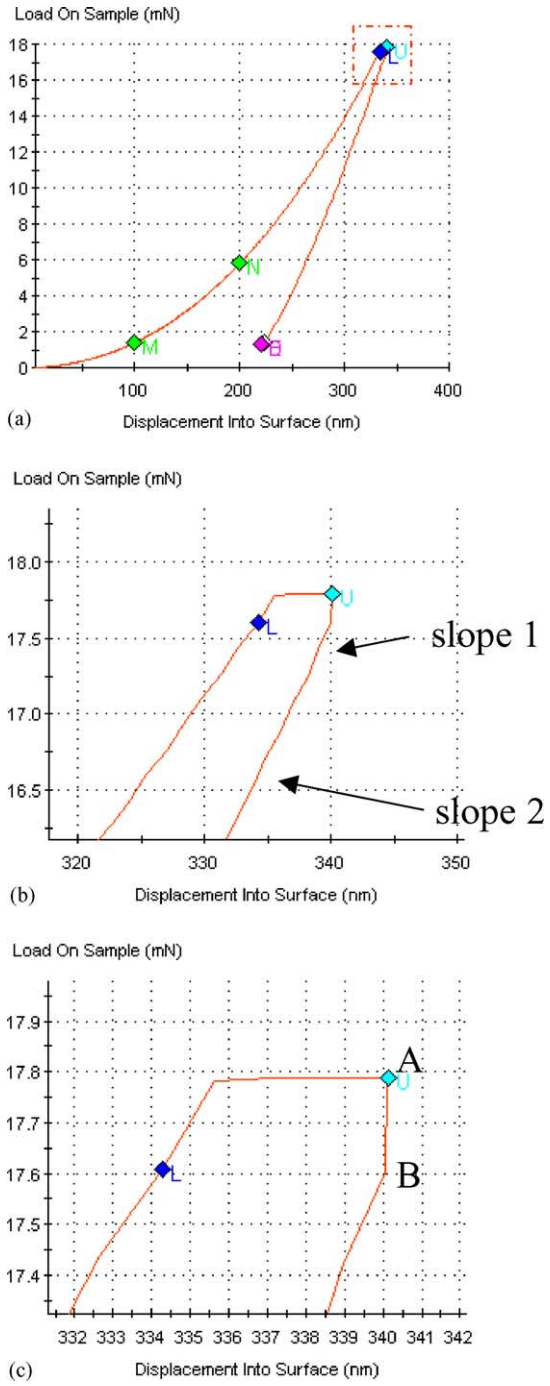

Fig. 8. A typical force vs. indent depth curve.

test. Hence, the elastic modulus of the thin film materials for various different thicknesses was measured, as shown in Fig. 5. The indenter load is increased from zero to a certain maximum value P_{max}, and then gradually decreased to zero. The elastic modulus changes drastically in the beginning due to the surface profile of the indentation point. According to the substrate effect, the elastic modulus varies with the indent depth. A conservation rule of thumb is that the depth of the contact should be less than 10% of the thin film thickness, thoughin some materials have been claimed for depths of up 25% [16]. Thus, in fair agreement as mentioned previously, the Young's modulus for SiO_2, Si_3N_4, Al and Ni under consider the range at 5 and 10% of each thickness are 71, 283, 72, 202 GPa, respectively.

In addition, the experiment results for bulk materials Si and Al is show in Fig. 6. The measured results in Fig. 6a

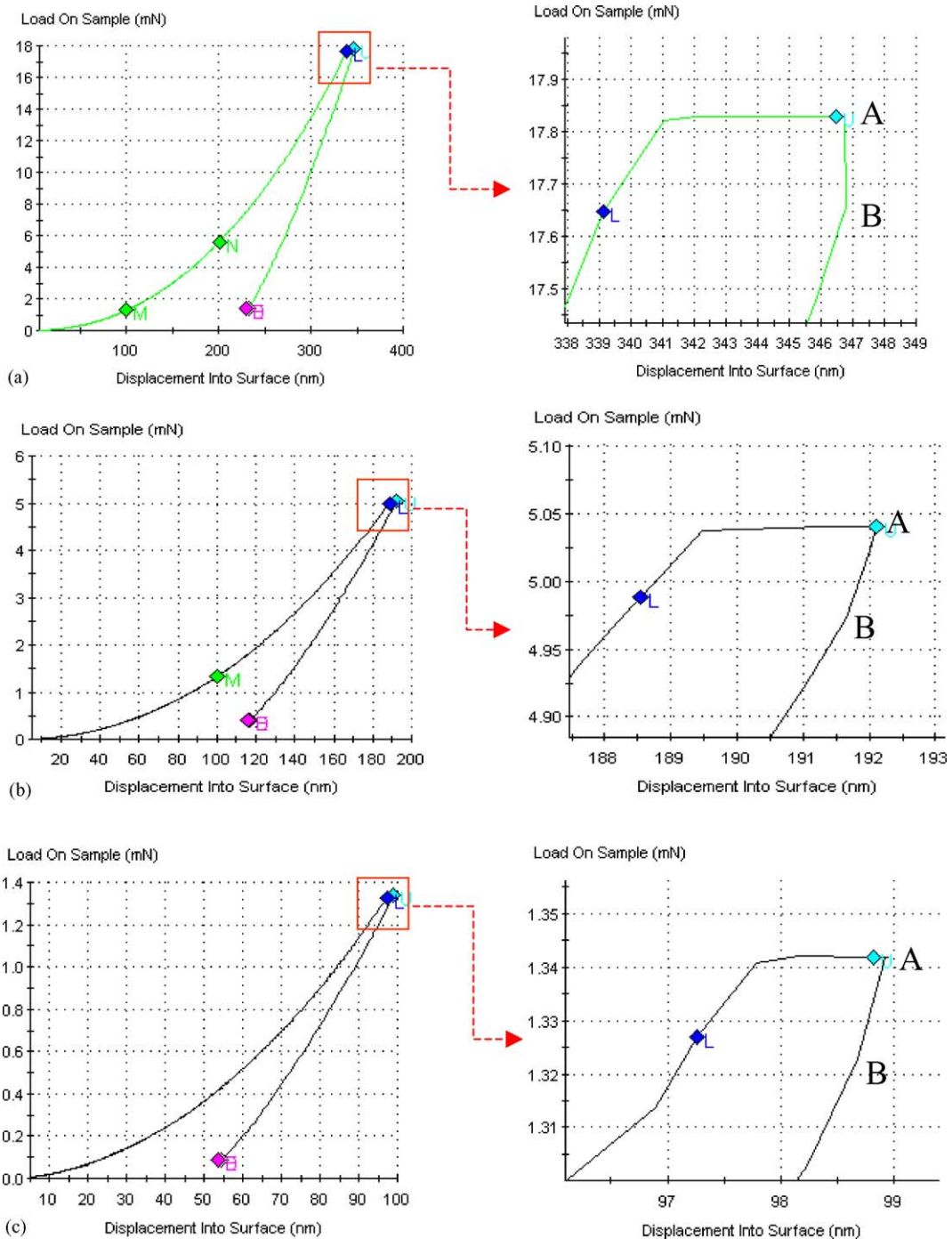

Fig. 9. The load–deflection curve of the SiO_2 thin film under three different indentation depths.

reveal that the elastic modulus of bulk Si is still increasing with indentation depth, although the substrate effect is no longer existed. Accordingly, the experimental results of the indentation test are influenced not only by the substrate effect. In addition, the measured results in Fig. 6b demonstrate that the elastic modulus of bulk Al becomes a constant value (E = 80 GPa) when the indentation depth larger than 200 nm. Consequently, the variation of the elastic modulus with the indentation depth is significantly difference between the ductile Al and the brittle Si materials.

4. Discussions

A physical model shown in Fig. 7 has been established in this study to explain the behavior observed in Fig. 6. Fig. 7 shows the indentation conditions on the contact interface that between tip and sample. During the loading and unloading processes, a normal force N resulted from the elastic restoring force of the sample will apply on the tip. Thus, a sliding contact friction f will apply on tip surface. In this case, the energy dissipation of the dynamic system due to the dry friction needs to be considered, so that the dynamic response z_0 in Eqs. (4) and (5) will be reduced. Apparently, the spring stiffness of the dynamic model in Fig. 2 will be increased if the dry friction is not considered. As the indent depth is increased, the dry friction is increased yet the dynamic response z_0 is decreased.

The types of friction between the probe tip and the sample are mainly determined by the contact condition during the indentation test. As shown in Fig. 8a, a typical force versus indent depth curve is used to study the characteristic of contact friction during indentation. The curve is measured from the SiO_2 thin film. The region inside the dashed box on Fig. 8a is zoomed in Fig. 8b, and the dashed box on Fig. 8b is further zoomed in Fig. 8a. As indicated in Fig. 8b, the unloading curve consists of two segments with different slope, and the turning point is labeled as B. In the beginning of unloading, the probe tip contact with the test sample tightly. There is no relative motion at the contact surface. Hence, a static friction force f_s ($N(\cos\theta - \mu_s \sin\theta)$) which tangent to the contact surface is applied on the probe tip. As the unloading process continued, there is relative motion occurring at the contact surface. Thus, the probe tip will experience a kinetic friction force f_k ($N(\cos\theta - \mu_k \sin\theta)$). The existing of static and kinetic friction force explains that the measured load–deflection curve has two different slopes during unloading process. As the indent depth is increased, the normal load N applied on the probe tip is increased, thus, the static friction force f_s is also increased. To further verify this characteristic, the load–deflection curve of the SiO_2 thin film under three different indentation depths is recorded, as shown in Fig. 9. Apparently, the slope of segment AB is increased with the indent depth. The characteristic associated with the contact friction is further demonstrating the

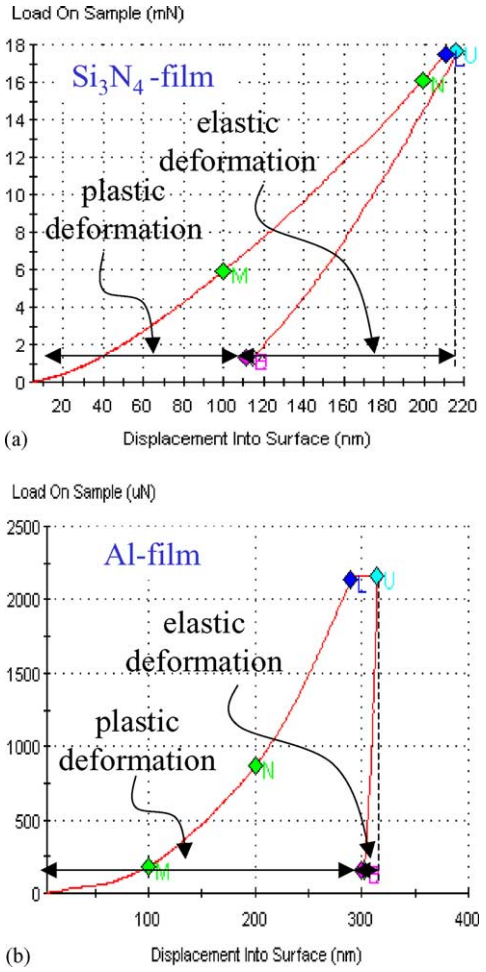

Fig. 10. The distribution of the elastic and plastic deformation regions for typical ductile (Al) and brittle (Si_3N_4) materials.

variation of the elastic modulus with the indent depth shown in Fig. 6.

The normal force N is resulted from the elastic restoring force of the sample. Fig. 10 shows the distribution of the elastic and plastic deformation regions for typical ductile (Al) and brittle (Si_3N_4) materials. It is obtained that the elastic deformation region for ductile material is much smaller than that of the brittle material. Hence, the normal force N caused by the ductile material is much smaller. Accordingly, the friction effect for brittle and ductile materials is different. In addition to the SiO_2, the indentation test on various thin films and bulk materials are performed and recorded in Fig. 11. The test samples contain the brittle materials such as SiO_2, Si_3N_4 and Si, and the ductile materials such as Ni and Al. As shown in Fig. 10, the load–deflection curve of all brittle materials has two segments with different slopes during unloading process. On the other hand, the load–deflection curve of all ductile materials has merely one segment during unloading process. In summary, the influence of the contact friction effect is more critical for the brittle material, as demonstrated in Fig. 6.

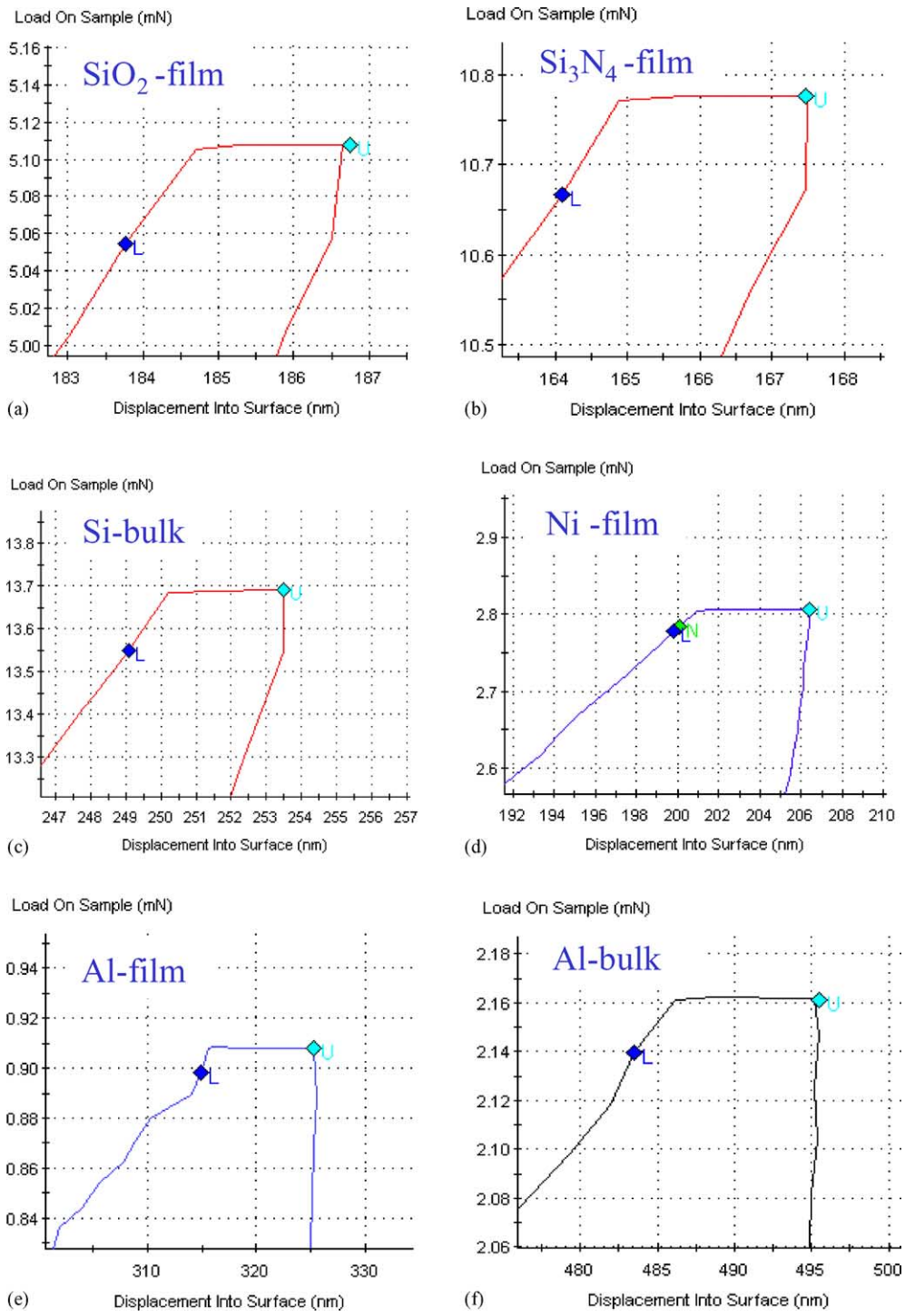

Fig. 11. The indentation test on various thin films and bulk materials.

5. Conclusion

This work demonstrates the effect of interface friction force during the indentation test. It is necessary to consider the influence of this effect when determining the thin film mechanical properties by indentation test. According to the experiment results, the static friction force f_s is increased with the indentation depth. Hence, the friction effect is influenced by the indentation depth. In addition, the friction effect for brittle and ductile materials is different. The interface friction force is more significant for the brittle material due to its larger elastic restoring force. Hence, the effect of friction force caused by the brittle material is large than that of ductile material. Consequently, the ignorance of the friction

effect may lead to significant error when extracting elastic modulus of thin films from the indentation test.

Acknowledgements

This project was (partially) supported by Ministry of Economic Affairs, ROC under No. 91-EC-17-A-07-S1-0011 and National Science Council of Taiwan under grant of NSC-92-2212-E-007-052. The authors would also like to appreciate the NSC Central Regional MEMS Center (Taiwan), the Nano Facility Center of National Tsing Hua University, and the NSC National Nano Device Laboratory (NDL) in providing the fabrication facilities.

References

[1] H.D. Espinosa, M. Fischer, E. Herbert, W.C. Oliver, Identification of residual stress state in an RF-MEMS device, www.mts.com/nano/MEMS_development.htm.
[2] M. Qin, M.C. Poon, C.Y. Yuen, A study of nickel silicide film as a mechanical material, Sens. Actuators A 87 (2000) 90–95.
[3] W.C. Oliver, C.J. Mchargue, Characterizing the hardness and modulus of thin films using mechanical properties microprobe, Thin Solid Film 161 (1988) 117–122.
[4] T.P. Weihs, S. Hong, J.C. Bravman, W.D. Nix, Measuring the strength and stiffness of thin film materials by mechanically deflecting cantilever microbeams, Mater. Res. Soc. Symp. Proc. 130 (1989) 87–92.
[5] S. Johansson, J.A. Schweitz, Fracture testing of silicon microelements in situ in a scanning electron microscope, J. Appl. Phys. 63 (1988) 4799–4803.
[6] R.P. Vinci, Bravman, Mechanical testing of thin films, in: Proceedings of the IEEE Transducers'91, Solid-State Sensor and Actuators, Yokohama, Japan, 1991, pp. 943–948.
[7] T.Y. Zhang, Y.J. Su, C.F. Qian, M.H. Zhao, L.Q. Chen, Microbridge testing of silicon nitride thin film deposited on silicon wafers, Acta Mater. 48 (2000) 2843–2857.
[8] C.J. Wilson, A. Ormeggi, M. Narbutovskih, Fracture testing of silicon microcantilever beams, J. Appl. Phys. 79 (1996) 2386–2393.
[9] K.J. Wahl, S.V. Stepnowski, W.N. Unertl, Viscoelastic effects in nanometer-scal contacts under shear, Tribol. Lett. 5 (1998) 103–107.
[10] S.A. Syed Asyf, K.J. Wahl, R.J. Colton, The influence of oxide and adsorbates on the nanomechanical response of silicon surfaces, J. Mater. Res. 15 (2000) 546–553.
[11] M.M. Chaudhri, A note on a common mistake in the analysis of nanoindentation data, J. Mater. Res. 16 (2001) 336–339.
[12] M.T. Kim, Influence of substrates on the elasticreaction of films for the microdentation tests, Thin Solid Films 283 (1996) 12– 16.
[13] W.C. Oliver, G.M. Pharr, An improved technique for determining hardness and elastic modulus using load and displacement sensing indentation experiments, J. Mater. Res. 7 (1992) 1564–1583.
[14] S.A. Syed Asyf, K.J. Wahl, R.J. Colton, Nanoindenation and contact stiffness measurement using force modulation with a capacitive load–displacement transducer, Rev. Sci. Inst. 70 (1999) 2408–2413.
[15] B. Borovsky, J. Krim, Measuring nanomechanical properties of a dynamic contact using an indenter and quartz crystal microbalance, J. Appl. Phys. 90 (2001) 6391–6396.
[16] G.M. Pharr, W.C. Oliver, Measurement of thin film mechanical properties using nanoindentation, MRS Bull. 17 (1992) 28–33.

Biographies

Chingfu Tsou received the MS, and PhD degrees in power mechanical engineering from National Tsing Hua University (NTHU), Hsinchu, Taiwan, Republic of China, in 1998 and 2003, respectively. Currently, he is an associate professor of the Department of Automatic Control Engineering, Feng Chia University, Taiwan, and has more than 2 years of working experience in the field of MEMS. His research interests include MEMS devices and systems, as well as MEMS/IC packaging technology.

Changchun Hsu was born in Pingtung, Taiwan, in 1980. He received the BE degree from National Tsing Hua University in 2002. He is currently working towards his ME degree in power mechanical engineering, National Tsing Hua University, Taiwan. His main interests are the nanoindentation test.

Weileun Fang received his PhD degree from Carnegie Mellon University in 1995. His doctoral research focused on the determining of the mechanical properties of thin films using micromachined structures. In 1995, he worked as a postdoctoral research at Synchrotron Radiation Research Center, Taiwan. He is currently a professor at Power Mechanical Engineering Department and MEMS Institute, National Tsing Hua University, Taiwan. His research interests include MEMS with emphasis on novel microfabrication process, microoptical systems, microactuators, and the characterization of the mechanical properties of thin films.